Asia Pacific Research Initiative for Sustainable Energy Systems 2014 (APRISES14)

OCEAN THERMAL ENERGY CONVERSION (OTEC)

Task 6.1

Prepared For
Hawaii Natural Energy Institute

Prepared By
Makai Ocean Engineering

July 2018

HNEI
Hawaiʻi Natural Energy Institute
University of Hawaiʻi at Mānoa

OCEAN THERMAL ENERGY CONVERSION (OTEC)

Prepared For

HAWAII NATURAL ENERGY INSTITUTE

RICK ROCHELEAU

1680 East West Road, POST 109

Honolulu, HI, 96822

USA

Prepared By

MAKAI OCEAN ENGINEERING

PO Box 1206, Kailua, Hawaii 96734

July 2018

1. INTRODUCTION

Since 2009, Makai Ocean Engineering, Inc. has been conducting research in support of developing Ocean Thermal Energy Conversion (OTEC) for both US Navy and commercial applications. Makai's OTEC work is conducted at the Ocean Energy Research Center (OERC), located within the Natural Energy Lab of Hawaii Authority (NELHA) in Kailua Kona, Hawaii. Makai's research at the OERC is focused on: 1) new heat exchanger designs and fabrication methods, 2) evaluation of heat exchanger performance, and 3) corrosion testing.

Makai's initial heat exchanger design concept was a foil-fin heat exchanger (FFHX) in which a sheet of aluminum fins was sandwiched between two sheets of titanium foil. The aluminum fins would improve the ammonia-side heat transfer while the titanium foil provided corrosion resistance in seawater. Makai built and tested several epoxy-bonded versions of this heat exchanger and, because epoxy is incompatible with ammonia, began to develop a laser-welded version. However, concerns regarding the reliability of the foil-fin weld and an analysis that suggested for an OTEC heat exchanger it is more effective to increase heat transfer area instead of heat transfer efficiency, led Makai to develop thin foil heat exchangers (TFHX). The TFHX is constructed from titanium and utilizes a proprietary process to form the working fluid and seawater passages.

Makai constructed two 100-kW scale TFHXs and tested each as a condenser and as an evaporator. Changes in the plate geometry led to improved performance. When scaled to 2MW for comparison to previously tested heat exchangers, the TFHX performance exceeded that of the previously tested heat exchangers in terms of heat exchanger pressure and required seawater pumping power for the same duty. However, using prototype-scale fabrication costs, the TFHX is 2-3X more expensive than existing heat exchangers. Makai's future development targets improving performance, compactness, and cost competitiveness of the TFHX.

Makai continues to conduct corrosion testing. Aluminum plate samples remain in the warm and cold multi-column imaging racks (MCIR) with acid and hypochlorite treatments. TFHX samples have also been tested in the cold seawater MCIR. Aluminum box beam samples also remain in warm and cold seawater; as of July 1, 2018, the box beam samples have been tested for almost 9 years.

This report summarizes the work performed between February 2016 and July 2018 specifically pertaining to:

- TFHX development

- 100-kW testing station

- TFHX performance and economic analysis

- Corrosion testing from February 2016 to July 2017

2. TFHX DEVELOPMENT AND FABRICATION

TFHX development and fabrication is performed in a 19' X 16' Class 10,000 cleanroom located within the Water Quality Laboratory building at NELHA.

The TFHX has had a production success rate of over 99.99%. The primary focus of TFHX development was determining the relationship between the pressure rating and parameters in the fabrication process. These parameters must be balanced to produce ammonia channels that allow adequate flow inside the heat exchanger and provide adequate seawater side convection at the 250 psi pressure rating. Makai was able to predict the burst pressure of TFHX samples and ammonia passage widths based on two fabrication parameters. This predictive capability means TFHX plates can be readily customized for different applications.

OTEC applications require a pressure rating of 250 psi (1.45 safety factor applied to operational pressure of 170 psi). By changing fabrication parameters, ammonia passage widths can be varied from 0.2 mm to 1.1 mm while meeting the 250 psi pressure rating (Figure 1).
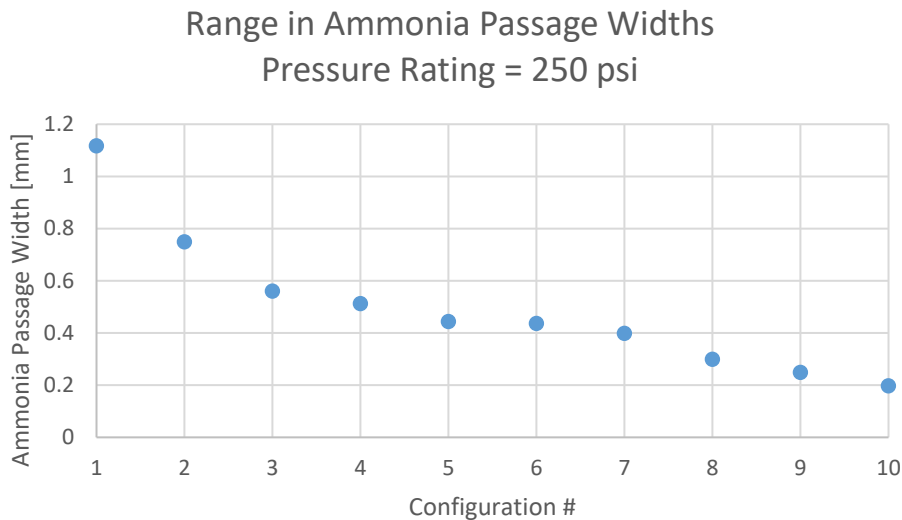
Range in Ammonia Passage Widths
Pressure Rating = 250 psi

Figure 1. Changes to fabrication parameters result in a range of available ammonia passage widths (0.2-1.2 mm) for the same pressure rating.

3. 100-kW TESTING STATION

Makai designed, constructed, and commissioned the 100-kW testing station to test the TFHXs. Testing at the 100 kW scale (vice the 2 MW scale) allows for more responsive design changes due to faster fabrication times for smaller sized heat exchangers but also provides adequate accuracy in data collection.

The primary purpose of the 100-kW station is to support performance testing of Makai's cross-flow and counter-flow TFHXs and other (to be developed) heat exchangers. This means the 100 kW station must accommodate at least four heat exchanger stations:

1) APV companion heat exchanger,
2) a horizontally-oriented, cross-flow TFHX,
3) a vertically-oriented, cross-flow TFHX, and
4) a vertically-oriented, counter-flow, water-to-water TFHX.

Except for the water-to-water TFHX, each heat exchanger must operate as a condenser and an evaporator, so the 100-kW station must support both evaporator and condenser configurations by opening/closing a few valves (instead of removal/reinstallation). Since multiple heat exchanger configurations (some not yet developed) are to be tested, the 100-kW station was designed to provide flexibility to test new designs and conduct new types of testing.

The heat exchangers are specified for 100 kW nominal duty, with a testing range of 40-160 kW. Ammonia and seawater systems were sized to accommodate the range in duty. In the seawater system, because the seawater supply pressure is set by NELHA, this meant using 6" piping to minimize frictional losses. In the ammonia system, this meant selecting 1½" vapor piping to limit ammonia vapor velocity to < 35 m/s and 1½" condensate piping to prevent bottling at the condenser exit. Also, new ammonia pumps were purchased to accommodate the required ammonia flow rate range; the old pumps were sized for a 100-kW propane system and were oversized for ammonia.

Incorporating lessons learned from the heat exchanger testing tower, the new 100-kW station is enclosed, shaded, and humidity controlled to minimize environmental effects on testing and to protect the system components from the environment. The TFHX housing is also insulated to further minimize environmental heat transfer. The enclosure also provides a safety barrier in the event of an ammonia release. Accessibility to valves, gauges, sensors, pumps, ports, and the TFHX was incorporated into the design.

The secondary purpose of the 100-kW station is to test equipment and systems that may be used in a future OTEC system. For example, an ammonia sensor in the seawater discharge and an atmospheric (inside the enclosure) ammonia sensor is part of the safety system. The use of ammonia sensors is new to Makai and provides a test of the efficacy and practicality of ammonia detection sensors.

The 100-kW testing station can be divided into 10 subsystems:

1. Ammonia System – ammonia piping, pumps, valves

2. Seawater System – seawater piping and valves
3. Data Acquisition and Instrumentation – ammonia and seawater sensors, data acquisition system, and controls
4. Power and Conduit – instrument (DC) and equipment (AC) power and the conduit
5. Safety System – deluge components, ammonia detection sensors, and emergency buttons
6. Flushing System – freshwater piping for heat exchanger flushing
7. Ammonia Purging – purge port locations
8. Ammonia System Evacuation and Charging System – vacuum connections, vacuum pump staging, and connections for system charging
9. TFHX Housing – housing design
10. Infrastructure – concrete pad, enclosure, and tent

Each subsystem was described in detail in "MA1277_AMDT01 Deliverable 1.1 Report".

Construction of the 100-kW station started in October 2017. The seawater system was installed first because the headers lie underneath the concrete pad. The major components of the ammonia system (tanks, pumps, APV companion heat exchanger) were installed after the concrete work was complete. Some issues with misalignment in the ammonia piping in the off-site fabricated pieces were resolved with adjustments during the on-site final welding. Instrumentation and safety systems were installed in parallel to the ammonia system construction. The 100-kW station was completed in February 2018.

Figure 2. 100-kW station was completed in February 2018.

Commissioning and shakedown testing followed after construction completion. Commissioning tasks were divided by system – ammonia, seawater, data acquisition and instrumentation, control program, and safety system.

The ammonia system was evacuated and purged with nitrogen several times before being evacuated to 450 micron in preparation for ammonia charging. Vacuum was maintained over two days to ensure there were no leaks. It is essential to remove oxygen and non-condensable gases from the ammonia system. Trace amounts of oxygen pose a risk of stress corrosion cracking in the piping while non-condensable gases may adversely affect heat exchanger performance by raising heat exchanger operating pressure. Once the system was evacuated and no leaks were identified, the system was charged with ~ 100 lbs of ammonia.

In the ammonia system, both feed and recirculation pumps were verified to function at frequencies from 0-55 Hz. We did not have to adjust the backpressure on the pumps.

The seawater system was tested to determine the maximum flow rate through the system and to characterize seawater control valves. The flow rate depends on the pressure drop through the seawater system and NELHA's supply pressure. The maximum cold and warm seawater flow rate through the TFHX was 242 gpm and 235 gpm, respectively. This flow rate was sufficient for the expected testing range. Directing seawater through the HX Testing Facility could have increased the maximum flow rate, but it was not necessary.

The seawater control valves exhibited significant hysteresis and sensitivity/deadband issues which limited the precision and responsiveness that we could control seawater flow rates during testing. The control valve could not make small incremental movements; i.e., a command to go from 12% to 12.1% open resulted in no physical movement. Typically an incremental change of 2% was required before an actual movement occurred – and the resulting flow rate was much higher than originally intended. Furthermore, going from 12% to 14% frequently resulted in a different flow rate than if the valve were moved from 16% to 14%. This meant, to make adjustments to seawater flow rates, the control program had to close the valve 10% and then open to the new requested position. Flow control was more reliable if the valves were always moved in the same direction.

In the data acquisition and instrumentation system, all sensors were calibrated and verified to read as expected. Coriolis flow meters were placed in series and compressed air at 0.01 kg/s was passed through both sensors. Sensors read within 1%, which was in specification. Zero check and self-calibration was performed after the meters were installed and the system was charged with ammonia. Temperature sensors were calibrated using dT sensors and a temperature calibration fixture prior to installation. Ammonia pressure sensors were calibrated in place with a Rosemount pressure sensor. Seawater pressure sensors were "calibrated" periodically by taking static head measurements during periods of no flow.

Safety systems were verified to function by intentionally causing an emergency condition and observing that the required actions were taken. The triggers are: atmospheric ammonia concentration, seawater ammonia concentration, loss of electrical power, fire, and manual emergency stop. The responses for each trigger are the same except in the case of fire, the

ventilation fan does not turn on. The system responses are: turn off ammonia pumps, shut TFHX safety valves, start the deluge, start the ventilation fan, and send an alert email.

The 100-kW control program was tested over several days. Duty, LMTD, U-value, and h value calculations performed within the control program were independently calculated to verify accuracy. These calculations are used to evaluate heat exchanger performance.

The first level of testing verified manual controls (e.g., user inputs valve position and valve is observed to move to desired position). The next level of testing verified local controls (e.g., user inputs a setpoint such as seawater flow rate and the seawater control valve is adjusted until targeted flow is achieved). The final level of testing verified autonomous controls (e.g., the control program can set up conditions according to a test plan, collect a period of steady state data, and continue on to the point in the test plan).
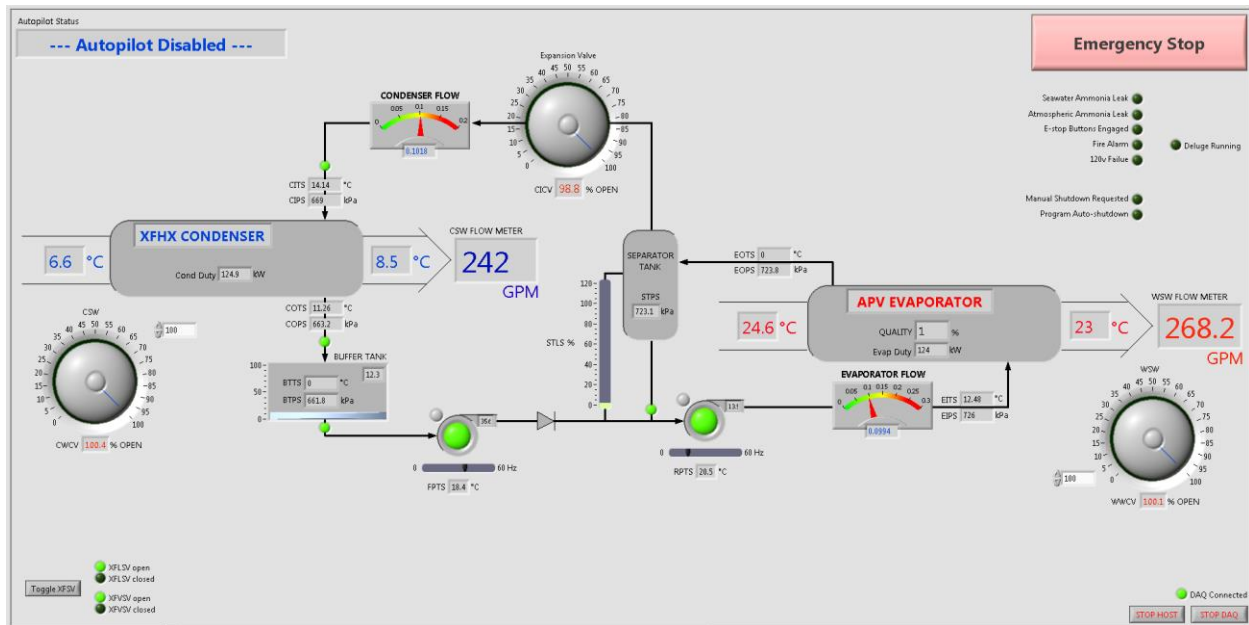

Figure 3. System overview page of the 100 kW Control Program. Seawater valves, the expansion valve, and feed and recirculation pumps can be controlled manually, locally, or autonomously.

4.   TFHX PERFORMANCE

A heat exchanger can be characterized by its seawater pressure drop, the overall heat transfer coefficient, seawater and ammonia heat transfer coefficients, heat exchanger operating pressure, power density, size, and cost. The relative importance of each characteristic is determined by the application.

Compared to previously tested heat exchangers at the OERC, the TFHX is a compact, efficient heat exchanger. The TFHXs were tested at energy densities (defined as duty/heat transfer area) from 11.0 kW/m^2 to 36.3 kW/m^2.

Table 1. Range in energy density for heat exchangers tested at the OERC

		Energy Density Range [kW/m^2]
Condenser	**TFHX1**	12.2 – 36.3
	TFHX2	11.1 – 34.5
	APVc	7.3 – 14.6
	ETHX	9.1 – 18.3
Evaporator	**TFHX1**	12.0 – 30.4
	TFHX2	11.0 – 28.0
	APVe	5.4 – 10.8
	BAHX3	11.1 – 22.2

In order to make fair comparisons of seawater pressure drop, overall heat transfer coefficient, or seawater/ammonia heat transfer coefficients the heat exchangers must be scaled to the same duty and energy density.

The TFHX condenser was scaled up to compare the overall heat transfer coefficient to that of the APVc at an energy density of ~12 kW/m^2 and a duty of 2.5MW and the ETHX at an energy density of ~12 kW/m^2 and a duty of 2 MW (Figure 4). Both TFHXs had U-values ~1.5X higher than that of APVc and ETHX at the same seawater pumping power (through the heat exchanger). This improvement can be traced to the improvement in seawater convective coefficient (Figure 5) and the ammonia condensation coefficient (Figure 6).

Similarly, the TFHX evaporator was scaled up to compare the overall heat transfer coefficient to that of the APVe at an energy density of ~ 11 kW/m^2 and a duty of 3 MW and the BAHX3 at an energy density of ~11 kW/m^2 and a duty of 1.5 MW (Figure 7). Both TFHXs had U-values higher than APVe but lower than BAHX3 for the same seawater pumping power. The seawater convective coefficients are about the same for all four evaporators (Figure 8); the difference is in the ammonia-side heat transfer coefficient (Figure 9). BAHX3's ammonia heat transfer coefficient is 1.75X higher than TFHX1 and comparable to TFHX2 at lower energy density, but 1.2X higher than TFHX2 at higher energy densities.
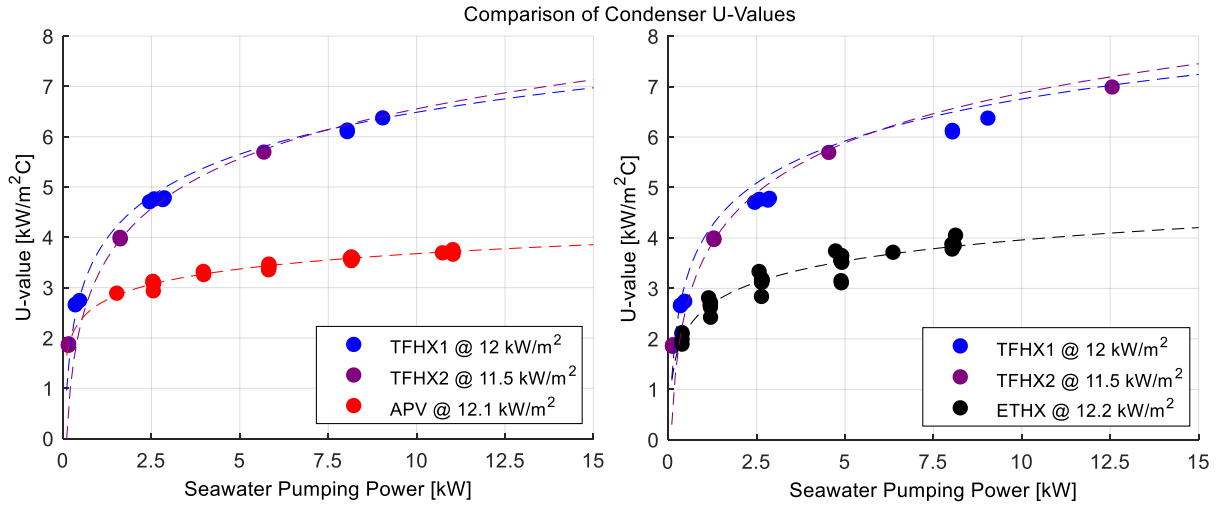
Figure 4. U-value vs Seawater Pumping Power comparison. TFHX's U-value is ~ 1.5X that of APVc or ETHX for the same seawater pumping power (through the heat exchanger only). Comparison with APV is scaled to 2.5 MW and comparison with ETHX is scaled to 2 MW.
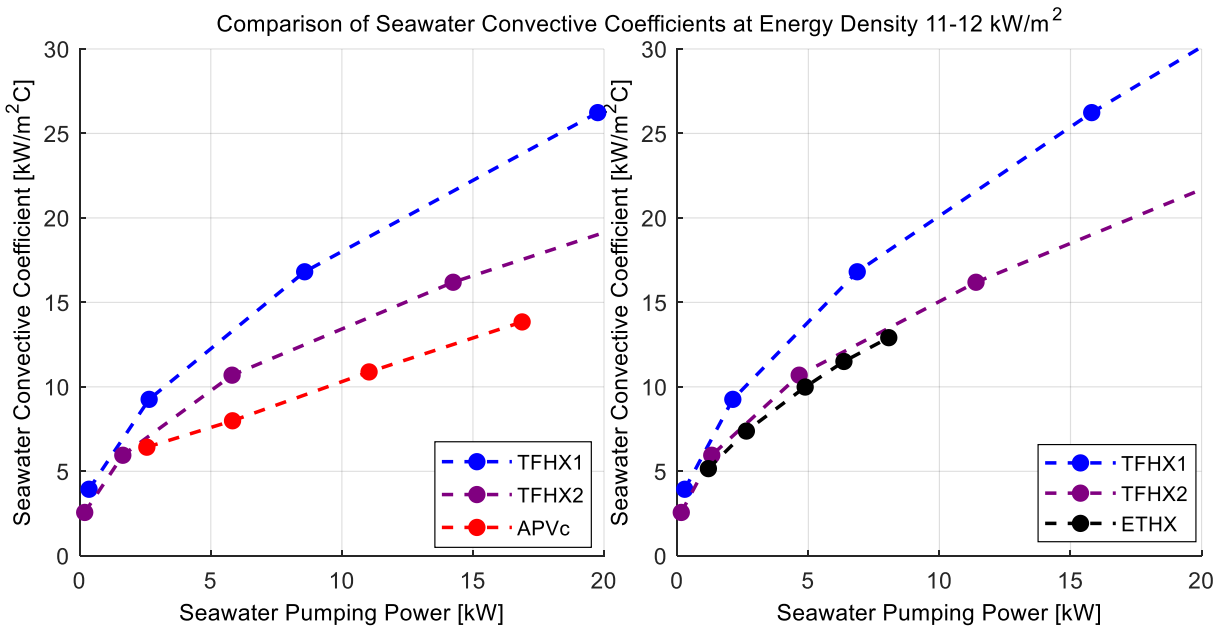

Figure 5. TFHX seawater convective coefficients are higher than APV and ETHX. Convective coefficients are plotted versus seawater pumping power to produce 2.5 MW for the APV comparison and 2 MW for the ETHX comparison at an energy density of 11-12 kW/m².
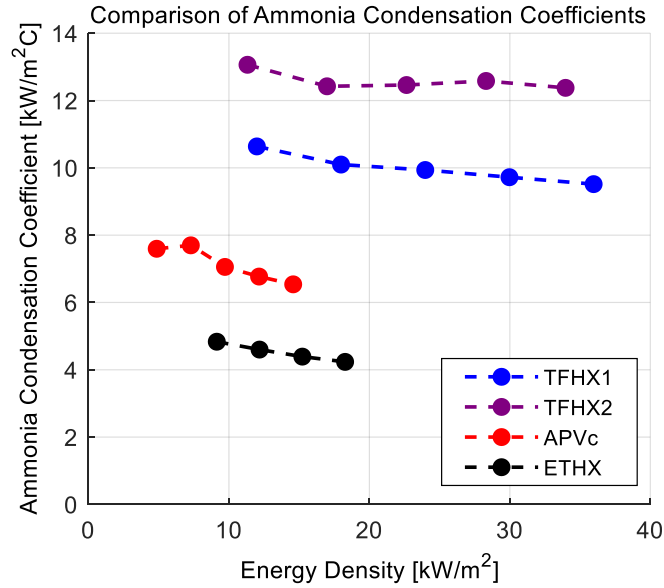
Figure 6. TFHX ammonia condensation coefficients are 1.5-3X higher than APV and ETHX at the same energy density.
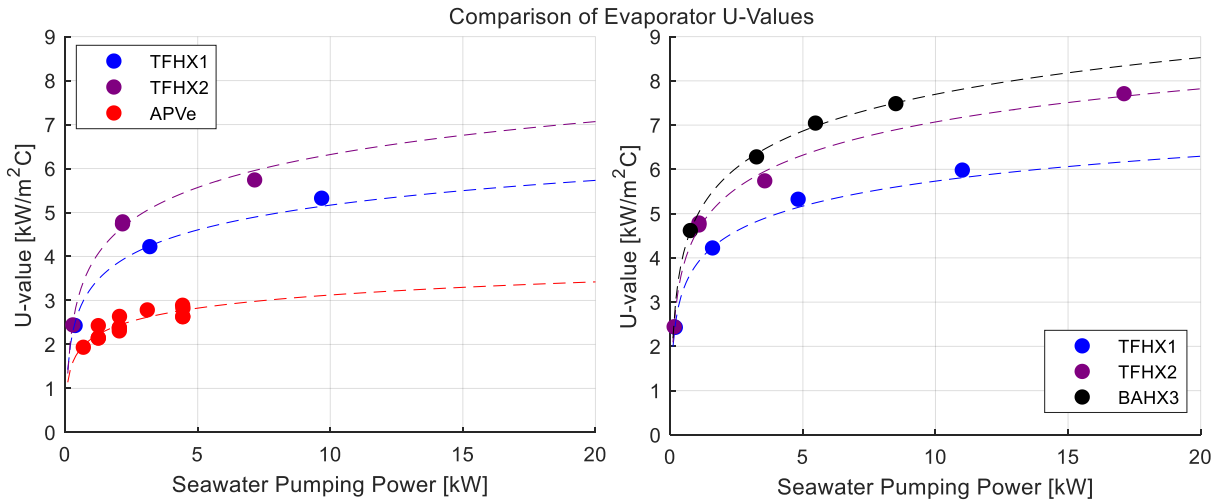

Figure 7. U-value vs Seawater Pumping Power comparison. TFHX U-value is ~ 1.2-2X that of APVe and ~0.7-0.9X that of BAHX3 for the same seawater pumping power (through the heat exchanger only).
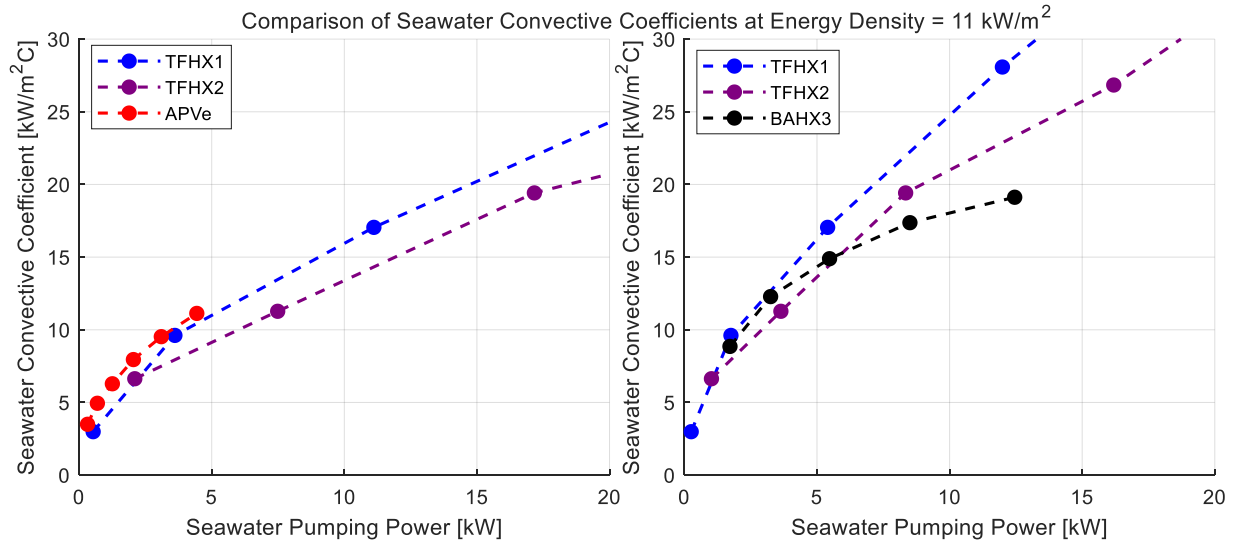
Figure 8. TFHX seawater convective coefficients are up to ~ 0.9X lower than APVe and comparable to BAHX3. Convective coefficients are plotted versus seawater pumping power to produce 3 MW for the APV comparison and 1.5 MW for the BAHX3 comparison at an energy density of 11 kW/m².
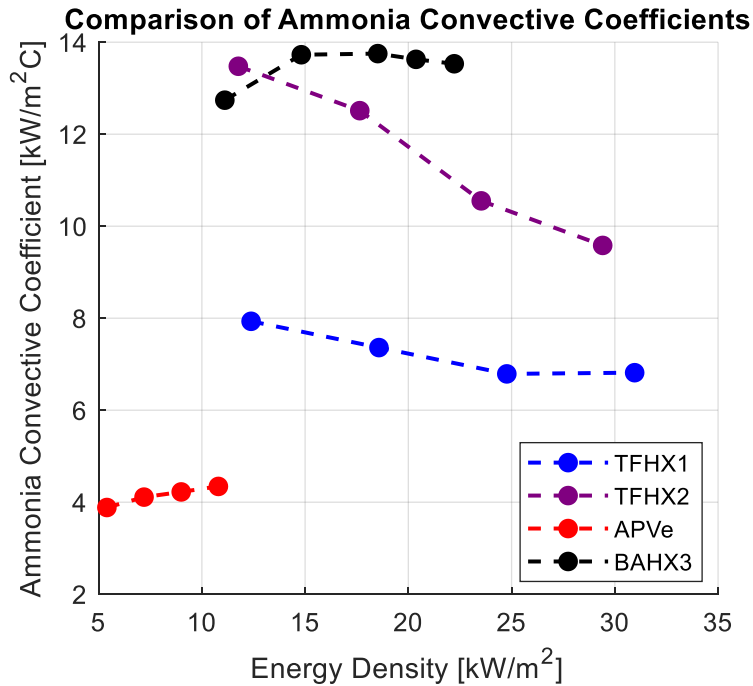

Figure 9. TFHX ammonia convective coefficients are ~2-3X higher than APV and ~0.5-0.85X lower than BAHX3 at the same energy density.

For an OTEC system, net power production depends on ammonia vapor mass flow rate, the differential pressure across the turbine, and the power required to pump seawater, which is a product of the required seawater flow rate and the pressure drop (through the heat exchanger and rest of the system). In the context of OTEC, a fair comparison will compare heat exchanger pressure at the same duty (ammonia vapor flow rate) and seawater pumping power; the energy density of a particular heat exchanger is not important in terms of thermal performance, but is important in terms of the overall system size.

The nominal duty for previously tested heat exchangers was 2 MW. For comparison to previously tested heat exchangers, the TFHX was scaled to 2 MW by adding plates; the number of plates required to attain 2 MW increases with decreasing power density (Table 2).

Table 2. Plates required for 2MW TFHX at different energy densities.

TFHX1 Condenser	**Energy Density [kW/m²]**	12.17	18.24	24.15	30.15	36.25
	# of plates for 2 MW	306	204	154	124	103
	Required HX area [m²]	164.38	109.68	82.82	66.32	55.17
TFHX2 Condenser	**Energy Density [kW/m²]**	11.11	16.96	22.81	28.65	34.50
	# of plates for 2 MW	316	207	154	123	102
	Required HX area [m²]	180.00	117.93	87.69	69.80	57.97
TFHX1 Evaporator	**Energy Density [kW/m²]**	11.96	18.18	24.22	30.35	
	# of plates for 2 MW	311	205	154	123	
	Required HX area [m²]	167.16	110.03	82.59	65.90	
TFHX2 Evaporator	**Energy Density [kW/m²]**	11.03	16.73	22.29	28.03	
	# of plates for 2 MW	319	210	158	126	
	Required HX area [m²]	181.33	119.55	89.74	71.36	

At an energy density of ~12 kW/m², TFHX operating pressure (for both condensers and evaporators) was better than the previously tested 2MW heat exchangers across the 0.5-10 kW range of seawater pumping powers (Figure 10 and Figure 11). TFHX maintains a favorable operating pressure while operating at a higher energy density.

Due to the compactness (i.e., high heat transfer area to volume ratio) of the TFHX (Figure 12), a 2 MW TFHX is 4-8X smaller in volume than the heat exchangers previously tested at the OERC (Figure 13). Using prototype-scale fabrication costs, the TFHX is 2-3X more expensive than the previous heat exchangers (Figure 14).
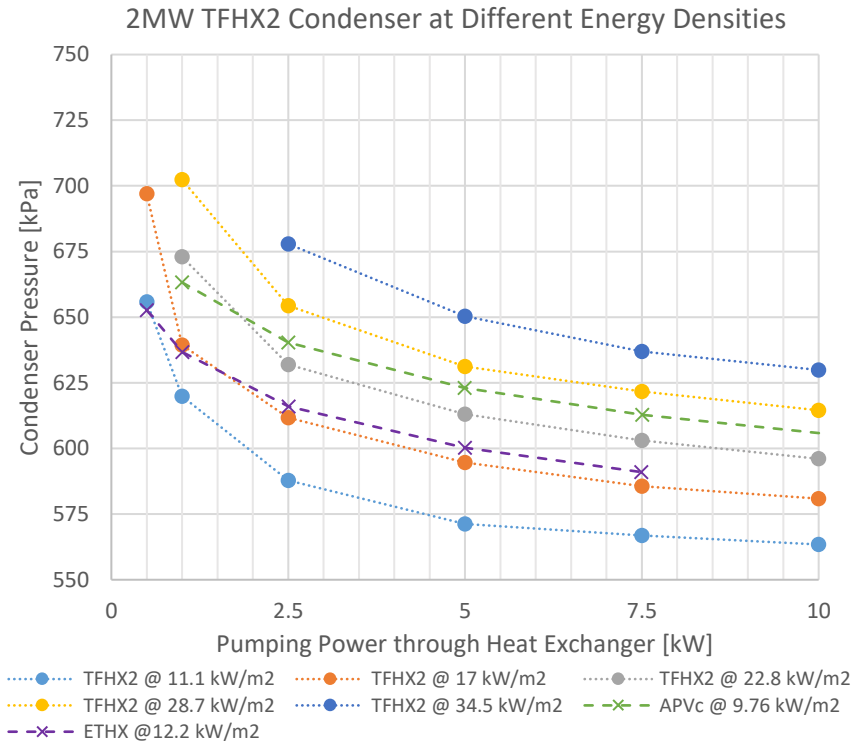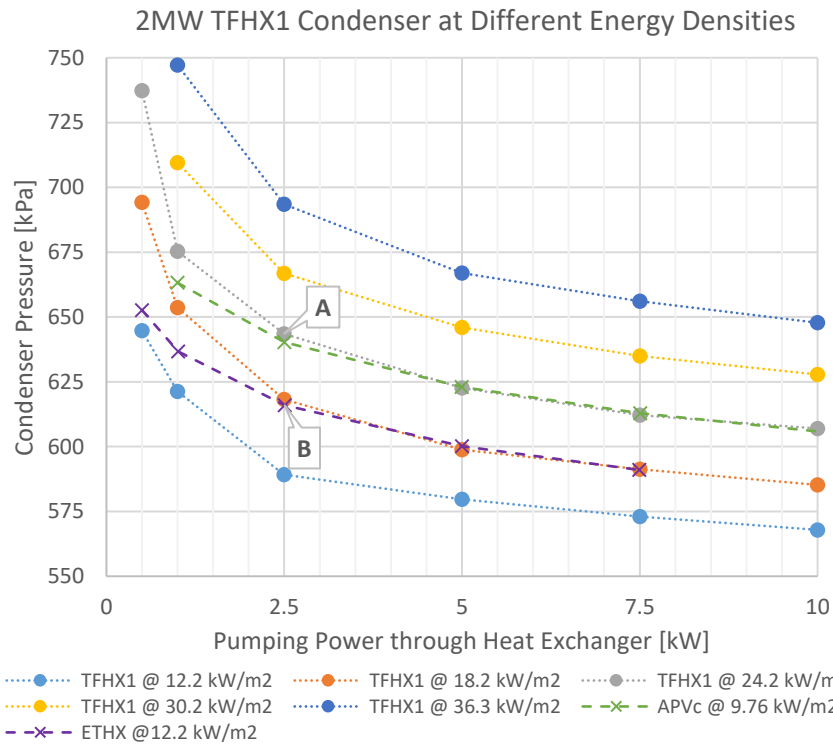
Figure 10. Comparison of condenser operating pressure versus seawater pumping power for 2MW TFHX condensers at various energy densities and 2MW APV and ETHX condensers. For the same seawater pumping power (through the heat exchanger only), the TFHX is capable of lower operating pressures at power densities up to 24 kW/m² compared to APVc (Point A) and power densities up to 18 kW/m² compared to ETHX (Point B).
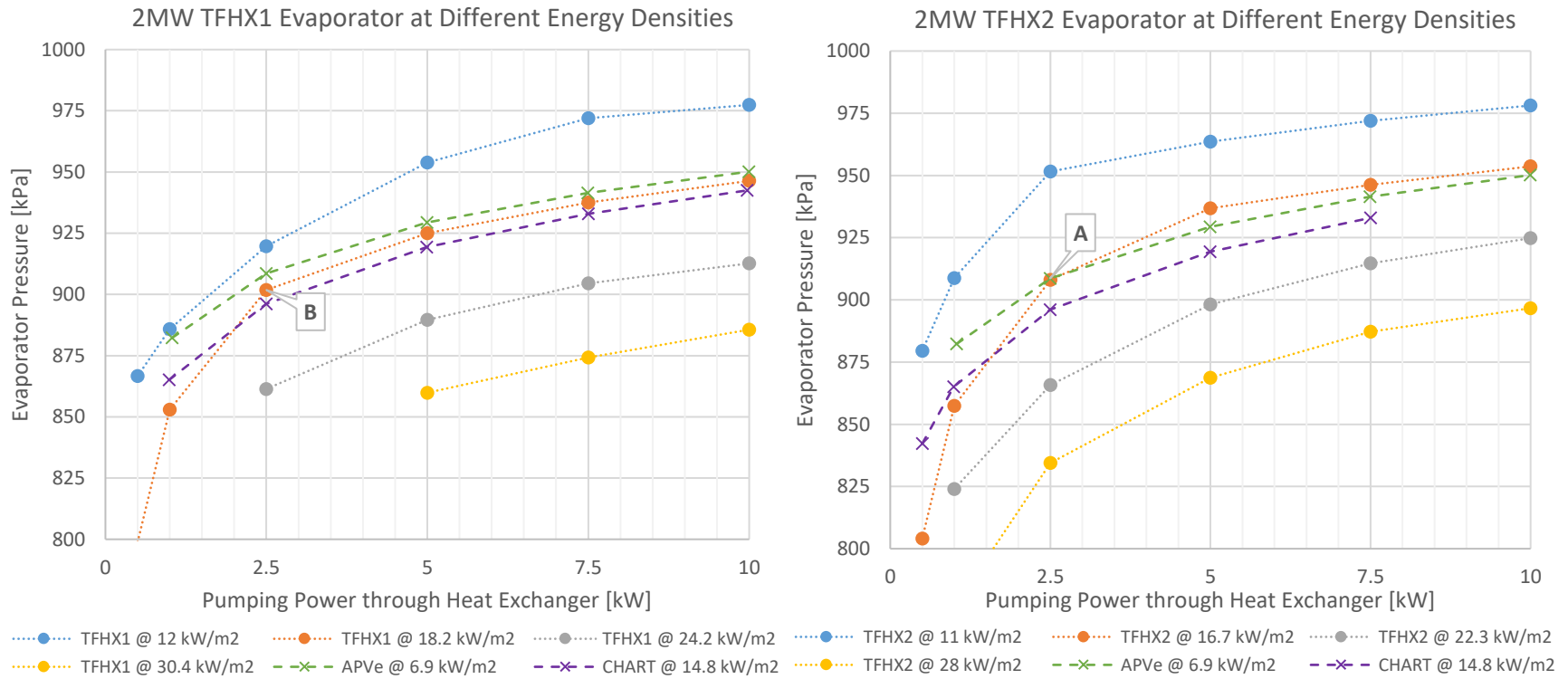
Figure 11. Comparison of evaporator operating pressure versus seawater pumping power for 2MW TFHX evaporators at various energy densities and 2MW APV and CHART evaporators. For the same seawater pumping power (through the heat exchanger only), the TFHX is capable of higher operating pressures at power densities up to 16 kW/m² compared to APVe (Point A) and at power densities up to 18 kW/m² compared to CHART (Point B).
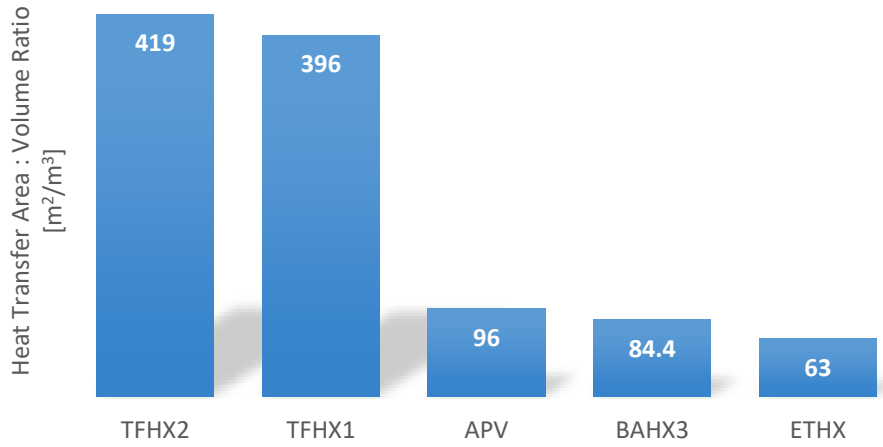
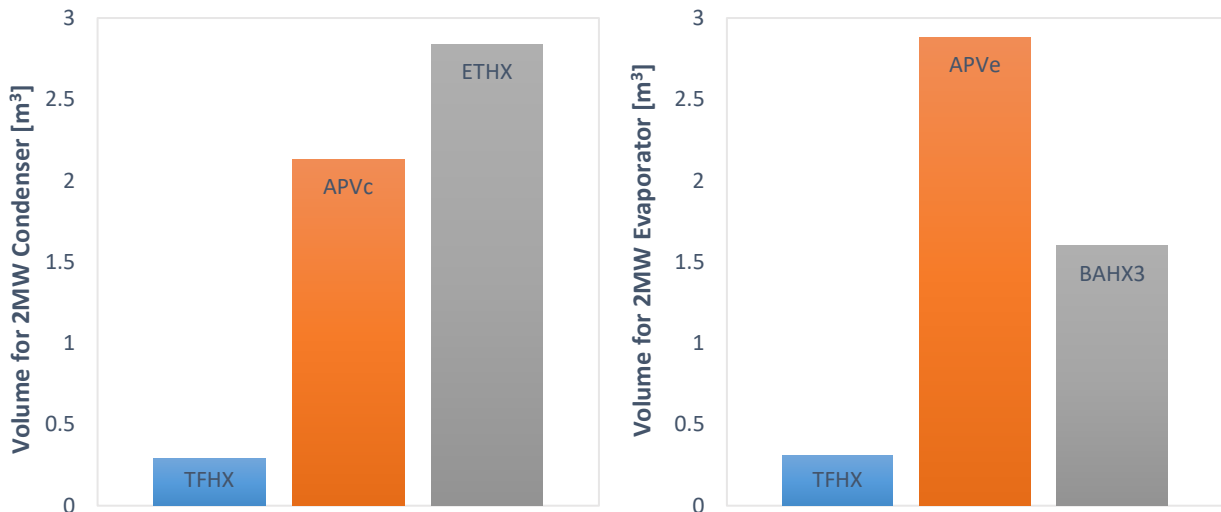*Figure 12. Comparison of heat transfer area to volume ratio for tested heat exchangers.*

Figure 13. Comparison of required volume for 2 MW heat exchanger

Figure 14. Comparison of estimated cost for 2MW heat exchanger.

5.   CORROSION TESTING

Corrosion testing is on-going and this section summarizes Makai's corrosion-related findings from February 2016 to July 2017 only.

As of July 2017, corrosion samples included box samples, representative heat exchanger samples, and plate, ultrasonic, and mini-FFHX samples in the Multi-Column Imaging Rack (MCIR).

5.1.   BOX COUPONS

Box coupons have been tested since 2009. The last removal and analysis of box coupons was performed in 2014, after 5 years of exposure in WSW, CSW, and DSW. Rack consolidation took place in 2015; a total of 5 columns of WSW samples, 2 columns of CSW samples, 1 column of WSW pre-treated samples, and 3 columns of DSW samples remain in testing.

Alloys have performed well in WSW. Large pits were identified on some samples after 2 years, but not on samples removed after longer exposure. The pits were attributed to manufacturing defects or bias in testing conditions and are not believed to be indicative of alloy performance in WSW.

Alloys have performed unpredictably in CSW. Alloys 1100 and 3003 have the least scatter. Although some Alloy 3003 samples had pits > 0.5 mm, most have performed well. Alloys 1100, LA83I, and LA83P had a few very poorly performing outlier samples, but in general, the weight loss results and pitting statistics followed a trend of increasing pits and pit depths with exposure time. Alloys 5052 and 6063 had highly variable performance; it is possible these alloys were subject to more manufacturing variability that affected performance.

Based on results from the 4-year samples, except for Alloy 6063, the WSW pre-treatment samples performed better than the CSW samples.

Alloys performed poorly in DSW. In addition to pitting, crevice corrosion was also severe for the DSW samples.

Removal of box coupons is not planned until the remaining samples have been tested for 10 years.

5.2.   REPRESENATIVE HEAT EXCHANGER SAMPLES

Six FSW tubular mini-HX samples were reallocated to Makai from a previous testing contract. Testing began on the samples in 2014. Of the two CSW samples, one received the WSW pre-treatment (CSW-1) while the other was directly exposed to CSW (CSW-2). CSW-1 has corrosion and the FSW pull out points on both upstream and downstream tubesheets. Corrosion product was observed after ~2 years of exposure. There is also crevice corrosion at the gasket interface on the downstream tubesheet of CSW-1. Heat exchanger designs must carefully consider interior low-flow areas when using materials susceptible to corrosion. CSW-2

does not have visible corrosion product but is covered with black biofouling spots. The tube interior walls on both CSW samples are also rough; it is difficult to tell whether the attachments are biofouling or corrosion product.

The four WSW mini-HX samples show no signs of corrosion product; however, biofouling is present on all samples. Biofouling has been worse on the upstream tubesheets compared with the downstream tubesheets. WSW-3 and -4 had a pattern on the interior tubewalls that was intended to enhance heat transfer; the pattern is no longer distinguishable, the tube walls appear to be covered with a fuzzy biofouling layer.

One mini-CHART sample has been exposed in WSW since December 2013. After 4 years of exposure, no noticeable change has been observed. No corrosion product is visible, small flecks on the upstream face may be biofouling. The window on the upstream face has been obscured by biofouling film.

5.3. FFHX COUPONS

FFHX corrosion sample testing began in June 2015. The first three samples were removed after 2 months due to corrosion at weld defects and at the gasket interface. Three additional samples were tested starting in September 2015 and removed in February 2017. At the time of removal, all FFHX samples were severely corroded. Corrosion that initiated at a weld defect progressed on the back side of the sample, corroding the aluminum fins to the extent that the fins detached from the titanium foil. Along some weld lines, enough corrosion product built up to push and eventually tear the fins from the foil along the weld line.
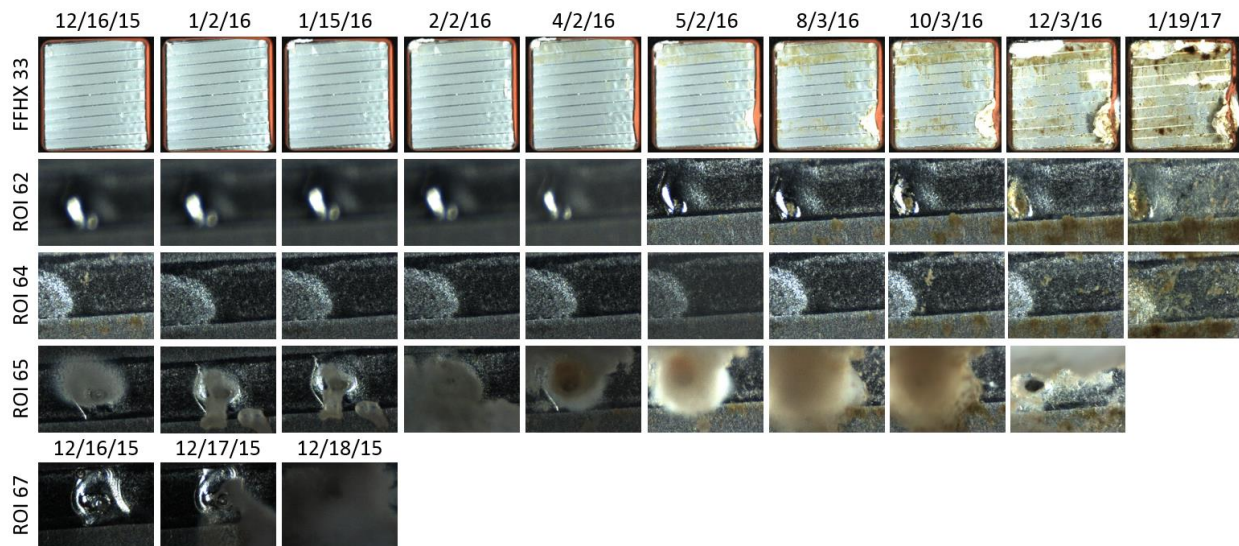

Figure 15. Sample was removed after 13 months. Three out of eleven weld lines had significant corrosion product and gasket corrosion was severe. Seawater was leaking out the back side due to gasket distortion from corrosion product.

FFHX corrosion testing emphasized the importance of reliable welds – defects most likely exposed the aluminum fins to seawater and began to corrode preferentially. For an OTEC

heat exchanger, any breach from seawater to working fluid is considered a failure of the heat exchanger and must be avoided.

5.4.   TFHX COUPONS

Five TFHX samples were installed in the CSW MCIR in July 2017. The TFHX samples utilize the same delrin frame as the ultrasonic testing samples; three samples fit in one MCIR column. One column of samples will receive hypochlorination treatment (daily, 100 ppb dosage) and the other column will be the control. In each column, at least one sample will have the back side of the sample (vice the front side) exposed to CSW. Each sample also has a small pinhole punched into the non-exposed side. If any holes develop on the exposed foil, it should leak into the expanded region and drip out the pin hole.

Because the TFHX is only fabricated from titanium, corrosion is not expected. However, biofouling testing can provide treatment options for OTEC heat exchangers. In addition, the long-term performance of the samples in flowing seawater – in terms of maintaining the ammonia channel width and fatigue performance – also provides important data. Upon flow initiation, the samples were observed bow outward due to exposure to pressurized seawater. The sample was also observed to vibrate (like a speaker diaphragm), with dominate frequencies of 15 Hz and 58 Hz; this can provide an unintentional, but useful, fatigue test. In an actual heat exchanger, the TFHX plates will be supported by the pressurized ammonia; however, ammonia pressure may fluctuate depending on the seawater temperatures, seawater flow rates, and ammonia duty.

Automated imaging will not be performed due to low image quality due to the highly reflective, uneven, and occasionally vibrating surface. Images will be taken periodically with a camera.

Control Samples

T4 – front   M4 – back

Hypochlorination Samples
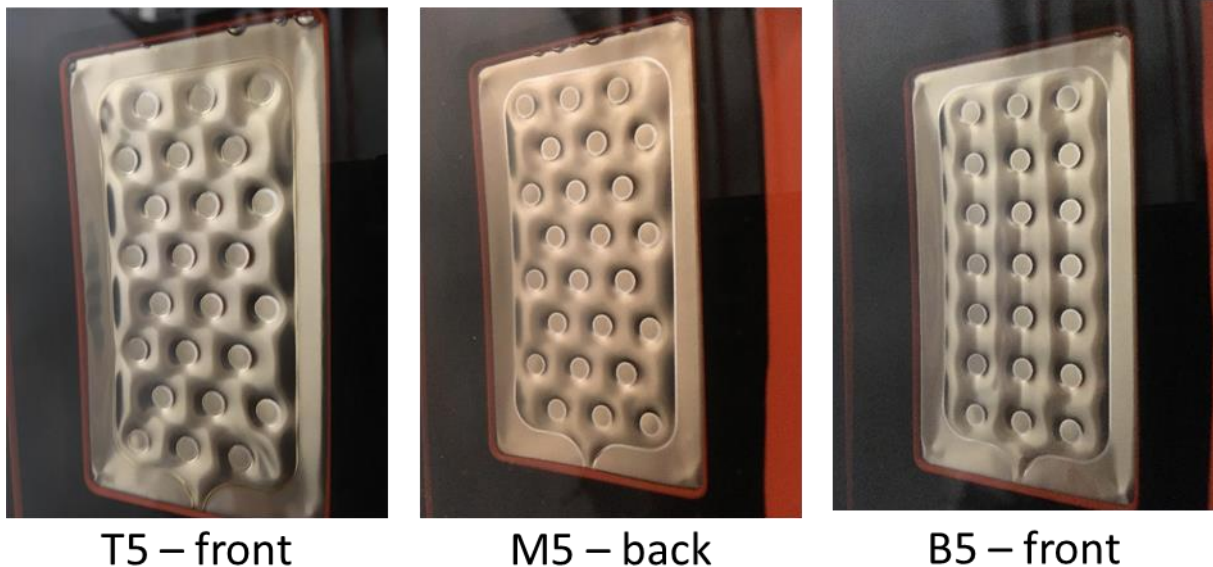
T5 – front   M5 – back   B5 – front

Figure 16. TFHX samples.

5.5.   PIT MITIGATION TREATMENTS

Makai has continued investigations into pit mitigation treatments in CSW in the MCIR. Acid treatments performed based on OCP-based intervals delayed the onset of pitting by over a year compared to the control sample. Pits appeared on the acid-treated sample only after a dry-out vice acid treatment was performed. Acid treatments performed on a 2-month interval were ineffective. Acid treatments have been observed to remove corrosion product buildup and biofouling. WSW pre-treatment delayed the onset of pitting by ~ 2 years. Ozone treatment was tested but increased pitting in CSW samples. Hypochlorite treatments (provided to ultrasonic samples) in CSW have maintained shiny, like-new sample surfaces.

Acid treatments were tested in WSW but results have been inconclusive as neither the control nor any of the treated samples had pits.

5.6.   BIOFOULING

Makai tested ozone, iodine, and chlorine dioxide treatments in addition to daily hypochlorite treatments for biofoulant control. Hypochlorite treatments are the most effective. As long as hypochlorite treatment is consistent, it is effective at preventing biofilm/biofouling; however, once biofilm begins to form (e.g., due to failure in the bleach delivery system), hypochlorination is does not remove the film and additional material can accumulate on the film. Although manual cleaning is effective at removing biofilm, it is time consuming and impractical for heat exchangers. Acid treatments and flow reversals remove most of the biofilm and can be implemented for a heat exchanger.

6. CONCLUSION

Makai's work has focused on developing, fabricating, and testing TFHX heat exchangers and corrosion testing.

Makai continues to conduct corrosion testing of aluminum alloys in 915-m cold seawater (DSW), 674-m cold seawater (CSW), and surface seawater (WSW). Previously, 5-year box beam samples were removed from DSW, CSW, and WSW. DSW and CSW samples had pits on nearly all samples. Pitting was most severe in DSW. Although some samples in CSW only had a few pits, alloy performance has been unpredictable; Makai does not recommend the use of untreated aluminum alloys for use in condensers. WSW samples had little to no pitting.

Aluminum plate samples remain in the warm and cold multi-column imaging racks (MCIR) with continued pit mitigation treatments. Treatments performed when open-circuit potentials indicate have been successful, although new pits have been observed if treatments have been delayed by as little as 48 hours.

Biofouling has become a problem for warm seawater samples. Any missed or reduced hypochlorite dosages lead to formation of a biofilm. Once the biofilm is formed, hypochlorination becomes less effective. Biofouling may be particularly severe at the OERC due to the age and condition of the warm seawater supply pipelines. Makai has previously found light penetration through PVC pipe walls is sufficient for algal growth. Much of the warm seawater distribution utilizes unshielded, above-ground, white, PVC pipes. Acid cleaning, flow reversals, or mechanical cleaning is required to remove the biofilm. Biofouling can cause microbially induced corrosion (MIC) and reduce heat transfer performance. Previous studies on ozone and iodine treatment were unsuccessful at preventing biofouling; consistent, reliable hypochlorination treatment with dosages based on the oxidation reduction potential (ORP) has been most effective at preventing biofouling.

FFHX and TFHX samples have also been tested in the cold seawater MCIR. As expected, FFHX samples have failed at burnthroughs where aluminum is in contact with seawater. TFHX samples are being tested in order to observe biofouling growth and fatigue response due to fluctuations in flow.

Makai's TFHX is fabricated using a Makai-developed proprietary process. The TFHX offers several advantages over Makai's previous heat exchanger concepts, the EBHX and FFHX (Table 3). Primarily, the manufacturing reliability made FFHX unfavorable while ammonia incompatibility and issues with epoxy creep and absorption eliminated the EBHX.

Makai fabricated and successfully pressure-tested the first 1.2-m long TFHX plate in November 2017 and continued on to fabricate twelve 1.2-m TFHX plates (6 plates per configuration) for performance testing.

Table 3. Comparison of EFHX, FFHX, and EBHX

	Working Fluid Compatibility	Manufacturing Reliability	Tine to Fabricate	Pressure Rating	Compactness
TFHX	No restrictions	High success rate	1st single plate, 5.5 man-hours*	Max tested pressure = 503 psi but pressure rating depends on fabrication parameters, >2100 psi possible	Currently ~400 m² of heat transfer area per m³, goal is >1000 m²/m³
FFHX	No restrictions	~ 60% of weld lines had defects	N/A	Max tested pressure = 185 psi	< 300 m² of heat transfer area per m³
EBHX	Incompatible with ammonia	High success rate	2 plates, 8.25 man-hours	Max tested pressure = 800 psi	< 300 m² of heat transfer area per m³

* Fabrication time for the first plate from start to finish, not including cleaning time. Future plates will utilize assemblyline style process and is expected to significantly reduce average fabrication time per plate.

In parallel with TFHX fabrication, Makai designed, constructed, and commissioned the 100-kW testing station to test TFHXs. The 100-kW testing station is a scaled at 100 kW nominal duty to allow for rapid fabrication times (fewer plates) while maintaining adequate instrument accuracy. The testing station has been designed with four "slots" for heat exchangers, but the ability to easily expand to include future stations was incorporated into the design concept. Minor issues during construction and commissioning were overcome and the 100-kW testing station was operational by March 2018.

Two configurations of TFHXs were fabricated and tested as both a condenser and an evaporator. TFHX2 performed better than TFHX1, driven by higher ammonia-side heat transfer coefficients even though the seawater convective coefficient was higher for TFHX1.

In order to compare the TFHXs to the previously tested heat exchangers at the OERC, the TFHXs had to be scaled up (by adding plates in parallel) so the duties were matched. It was also important to compare results based on seawater pumping power (vice the seawater pressure drop) because it accounts for the volume of water flow required for the duty. Compared to previously tested condensers, TFHXs had higher U-values for the same seawater pumping power (through the heat exchanger only). TFHX, as an evaporator, had higher U-values compared to APVe but lower than BAHX3.

In terms of an OTEC heat exchanger, the highest U-value may not always mean the best heat exchanger. An OTEC plant with the highest pressure drop across the turbine and the lowest seawater pumping power (for a fixed ammonia vapor flow rate, i.e., duty) will have a higher net

power. When evaluated in terms of heat exchanger operating pressure, at 2MW duty, the TFHXs have a better operating pressure at the same seawater pumping power *and* higher energy density compared to the previously tested heat exchangers.

However, using current fabrication methods, at the 2MW scale, the TFHX is 2-3X more expensive than competitor heat exchangers. Makai identified materials and labor (time) as the two major contributors to TFHX cost. With additional development, the cost to produce the current components could likely be reduced significantly (as much as 6X) when using high quantity fabrication techniques rather than prototyping.

Along with design changes to further improve performance and compactness, Makai's next TFHX also utilizes smaller, less costly components and is anticipated to require less time to fabricate. These improvements are targeted at making TFHX the obvious choice for not only OTEC, but many other heat exchanger applications.